


RESEARCH

Open Access



# Association of PD-1 + Treg/PD-1 + CD8 ratio and tertiary lymphoid structures with prognosis and response in advanced gastric cancer patients receiving preoperative treatment

Xu Liu<sup>1†</sup>, Danhua Xu<sup>1†</sup>, Chengbei Zhou<sup>2†</sup>, Yiqing Zhong<sup>1</sup>, Haigang Geng<sup>1</sup>, Chen Huang<sup>1</sup>, Yanying Shen<sup>3</sup>, Xiang Xia<sup>1</sup>, Chaojie Wang<sup>1</sup>, Chunchao Zhu<sup>1\*</sup> and Hui Cao<sup>1\*</sup> 

## Abstract

**Background** Recent studies have highlighted the distinct ratio of PD-1 + Treg/PD-1 + CD8 for prognosis prediction. However, it remains unclear about the association of this ratio and tertiary lymphoid structures (TLS) with prognosis and response to neoadjuvant or conversion therapy in advanced gastric cancer.

**Methods** Firstly, fresh postoperative samples from 68 gastric cancer patients in Renji Hospital were collected. Meanwhile, immune cell infiltration as well as clinical prognosis analysis were conducted. Subsequently, we further systematically evaluated flow cytometry analysis of tumor samples and TLS expression in 38 gastric cancer patients with different response situations after neoadjuvant therapy. Also, a Renji conversion therapy cohort including 10 patients with complete matching samples before and after treatment was established to receive RNA sequencing analysis and multiplex immunohistochemistry (mIHC) tests. The corresponding TLS score and immune cell infiltration were further compared based on therapeutic response variations.

**Results** In general, the ratio of PD-1 + Treg/PD-1 + CD8 > 1 could be regarded as an independent predictor of prognosis in advanced gastric cancer patients. Moreover, PD-1 + Treg/PD-1 + CD8 < 1 and high expression of TLS could indicate better neoadjuvant therapy response and extended survival time in advanced gastric cancer patients. Besides, PD-1 + Treg/PD-1 + CD8<sub>low</sub> & TLS<sub>high</sub> group could predict better progression free survival time (PFS) in complete response (CR) subgroup. In response group after conversion therapy, the number of PD-1 + CD8 + T cells

<sup>†</sup>Xu Liu, Danhua Xu and Chengbei Zhou contributed equally to this work.

\*Correspondence:  
Chunchao Zhu  
zcczmy@hotmail.com  
Hui Cao  
caohuishcn@hotmail.com

Full list of author information is available at the end of the article



© The Author(s) 2024. **Open Access** This article is licensed under a Creative Commons Attribution-NonCommercial-NoDerivatives 4.0 International License, which permits any non-commercial use, sharing, distribution and reproduction in any medium or format, as long as you give appropriate credit to the original author(s) and the source, provide a link to the Creative Commons licence, and indicate if you modified the licensed material. You do not have permission under this licence to share adapted material derived from this article or parts of it. The images or other third party material in this article are included in the article's Creative Commons licence, unless indicated otherwise in a credit line to the material. If material is not included in the article's Creative Commons licence and your intended use is not permitted by statutory regulation or exceeds the permitted use, you will need to obtain permission directly from the copyright holder. To view a copy of this licence, visit <http://creativecommons.org/licenses/by-nc-nd/4.0/>.

significantly increased, mainly occurring outside the TLSs. Meanwhile, the TLSs were also considerably activated as we could observe.

**Conclusions** This study underlined that combining PD-1 +Treg/PD-1 +CD8 ratio and TLS were significantly associated with prognosis and preoperative treatment response in advanced gastric cancer. Inspiringly, these indicators have the potential to elucidate the immune balance of advanced gastric cancer patients and can accurately guide subsequent therapeutic strategies.

**Keywords** Gastric cancer (GC), PD-1 +Treg/PD-1 +CD8 ratio, Tertiary lymphoid structure (TLS), Neoadjuvant therapy, Conversion therapy

## Background

Gastric cancer (GC), ranking fifth in incidence and fourth in mortality, still stands as a refractory public health menace worldwide [1]. Locally advanced gastric cancer is marked by tumors extending beyond the muscle layer or involving lymph node metastases, but without distant spread [2]. Treatment typically involves perioperative chemotherapy, immunotherapy, and surgical intervention. Neoadjuvant therapy aims to reduce the stage to increase surgical removal possibility. Besides, for patients with unresectable advanced gastric cancer, conversion therapy has been proposed as an emerging option [3–5].

Currently, immune checkpoint inhibitors (ICIs) have significantly revolutionized the treatment paradigm for numerous advanced cancers. Thereinto, PD-1 checkpoint blockade has gradually become the first-line treatment for GC [6, 7]. Recent researches have revealed that neoadjuvant chemoimmunotherapy significantly improves the prognosis of gastric cancer patients [8–10]. Despite the superiorities of this treatment, a large number of patients do not respond to anti-PD-1 therapy [11, 12]. Hence, to enhance the efficacy of neoadjuvant chemoimmunotherapy or conversion therapy in GC, there exists an urgent requirement to identify whether patients would benefit from the therapies mentioned above. A quantity of reports attempt to elucidate the changes in tumor microenvironment (TME) after neoadjuvant or conversion therapy from the perspective of immune microenvironment remodeling and upregulation of inhibitory immune cell subsets [13–16]. As per the latest reports, tumor infiltrative forkhead box P3-positive (FOXP3+) regulatory T cells (Tregs) might play a prominent role as an inhibitory factor [17–21]. It is widely acknowledged that PD-1 inhibitors mainly aim to improve anti-tumor immunity by releasing the brake of PD-1+CD8+T cells. Nevertheless, balance constraints are everywhere in nature. In gastric cancer, recent studies have revealed that the application of PD-1 inhibitors alone not only releases the anti-tumor activity of PD-1+CD8+T cells, but also discharges the inhibitory ability of PD-1+Tregs, which weakens the efficacy of PD-1 inhibitors to some extent. Shogo Kumagai et al. have elucidated that PD-1 blockade induces both recovery of dysfunctional PD-1+CD8+T

cells and boosted PD-1+Treg-mediated immunosuppression. They have presumed that a profound reactivation of effector PD-1+CD8+T cells rather than PD-1+Tregs by PD-1 blockade is essential for tumor regression [22–24]. However, there is still no consensus on the role of Tregs in the progression and prognosis prediction of gastric cancer, and the function of PD-1+Treg itself and its interactions with other cell subsets have not been fully elucidated [25–28]. As a pair of “balance factors”, the ratio of PD-1+Treg/PD-1+CD8 in bladder cancer is considered to be a predictor of the postoperative therapeutic effect in a recent research [29]. Despite that, the impact of this ratio on prognosis and response to preoperative treatment in different stages of gastric cancer has not been reported yet.

Tertiary lymphoid structures (TLSs) are transient ectopic lymphoid organs that develop in non-lymphoid tissues, such as sites of chronic inflammation and tumors [30, 31]. Structurally, TLSs are immune cell which aggregates with B cell lymphoid follicles surrounded by T cells. TLSs are generally accepted to play an essential role in antitumor immune response [32]. Undeniably, the presence of TLSs has been associated with a favorable prognosis and improved response to immunotherapy across many tumors including gastric cancer [33, 34]. In brief, higher TLS levels positively correlate with higher immunogenicity and immunoactivity in tumor microenvironment, demonstrating potential in predicting postoperative prognosis and immunotherapy response of GC. In view of the above theory, a recent research attempted to clarify the association of systemic inflammatory markers and TLSs with pathological complete response in GC patients receiving preoperative treatment [35]. In spite of that, few articles have explained the prognosis and therapeutic efficacy prediction of gastric cancer patients from the perspective of the combination of PD-1+Treg/PD-1+CD8 ratio and TLS.

This research retrospectively examined the immune cell infiltration by flow cytometry and conducted clinical prognosis analysis of fresh postoperative samples from 68 gastric cancer patients in our center thoroughly. Moreover, we further systematically evaluated the flow cytometry analysis of tumor samples and TLS expression in 38

advanced gastric cancer patients with different response situations after neoadjuvant therapy. Also, we centered on analyzing the mIHC results of paraffin sections from 10 pairs of advanced gastric cancer samples before and after conversion therapy. For these precious 10 pairs of samples, we also conducted transcriptome sequencing analysis. It has been found that the combination of PD-1+Treg/PD-1+CD8 ratio and TLS were significantly associated with prognosis and response to preoperative therapy in advanced gastric cancer patients. It is of great significance to predict their possible prognosis and response for preoperative therapy in the foreseeable future.

## Methods

### Study design and patients

This was a retrospective single-center study. Ethical approval for this study was provided by the ethical committee of our center. The participants provided their written informed consent to participate in this study. Firstly, the study reviewed 88 patients with gastric adenocarcinoma who experienced primary gastrectomy during the period spanning from May 2017 to December 2021 at the Department of Gastrointestinal Surgery, RenJi Hospital, School of Medicine, Shanghai Jiao Tong University. The inclusion criteria encompassed all the samples were definitely diagnosed as gastric cancer by Department of Pathology. All patients in this section have received conventional chemotherapy only, and not received postoperative immunotherapy yet. Moreover, among these people, Stage I cases have not received chemotherapy. We excluded the following types of patients: (1) patients without complete clinical information, postoperative pathological diagnosis, etc.; (2) patients with non-neoplastic resection; (3) patients who suffered from other primary malignant tumors; (4) primary tumor involving  $\geq 2$  regional sites; (5) unclear pathological types. Overall Survival time was defined as the interval between the gastrectomy and patient death or survival, and the final follow-up date was May 1, 2024, for all cases examined. After applying the eligibility criteria, we excluded 20 cases in the final study cohort. Among these excluded cases, out of which, 14 were loss to follow-up, 6 Stage I cases received chemotherapy. Then, 38 advanced gastric cancer patients who underwent neoadjuvant chemotherapy combined with immunotherapy were included in the study. The study reviewed patients with gastric adenocarcinoma who received neoadjuvant chemotherapy combined with immunotherapy followed by curative gastrectomy (R0 resection) during the period spanning from January 2021 to March 2023 at the Department of Gastrointestinal Surgery, RenJi Hospital. The time from the start of treatment to disease progression or death from any cause was defined as progression-free survival

(PFS). The final follow-up date was May 1, 2024, for all cases examined. Finally, 19 unresectable gastric cancer patients who underwent conversion therapy using immunotherapy plus chemotherapy with pre-conversion laparoscopic biopsy samples were included in the study. In this cohort, we excluded 9 cases which were pre-treatment slice unqualified. All of them experienced gastrectomy during the period spanning from December 2018 to July 2023 at the Department of Gastrointestinal Surgery, RenJi Hospital. The final follow-up date was May 1, 2024, for all cases examined. All patients received standard treatments according to the NCCN guidelines, and the immunotherapy involved above is limited to PD-1 inhibitors. The patients' tumor staging was in accordance with the American Joint Committee on Cancer (AJCC 8th edition) staging system.

### Pathological analysis

Formalin-fixed, Paraffin-embedded (FFPE) surgical samples were cut into serial sections with a thickness of 5  $\mu\text{m}$ . A total of 38 selected cases were immunologically stained for CD20 (1:150 dilution, RRID: ab64088, Abcam). TLSs were assessed morphologically based on Whole-Slide Image (WSIs) obtained. Briefly, for each patient, TLSs were initially identified in the WSIs using the ZEISS Axio Vert.A1 microscope system, which was presented as a lymphocyte aggregate on pathological images. To ensure the accuracy of TLSs identification, slides were independently evaluated by a senior pathologist. We categorized the amount of TLS according to previous researches as follows: 0=none, no TLS formation in the area adjacent to the tumor; 1=little, TLSs occupying an area of 1–10% of the tumor; 2=moderate, 11–50%; 3=abundant, > 50%. For survival analysis, we divided TLS into high (score  $\geq 2$ ) and low (score  $\leq 1$ ). Response Evaluation Criteria in Solid Tumors version 1.1 (RECIST 1.1) was applied as the criteria for calculating the immunotherapy response of patients. Responders were defined as patients with complete response (CR) or partial response (PR), while none-responders were defined as those with progressive disease (PD) or stable disease (SD). In addition, tumor regression grading (TRG) serves as a reference indicator. According to pathologic response of TRG, patients were labeled as responders (TRG=0–1) and none-responders (TRG=2–3) [36, 37].

### Multiplex immunohistochemistry staining

Slide images were acquired and analyzed using the Tissue FAXS (SL 7.1.120) and StrataQuest 7.1.129 software (TissueGnostics). mIHC staining was performed to visualise the expression of CD3, CD8, PD-1, CD20, FOXP3 in tumor tissues. The samples were collected within 30 min after tumor collection and fixed in formalin for 24–48 h. Dehydration and paraffin embedding were performed

using routine methods. Five consecutive Sect. (4  $\mu\text{m}$ ) were cut from paraffin blocks. Standard IHC procedures including dewaxing and rehydration of tissue sections, antigen retrieval, and blockade of endogenous peroxidase. Then sections were blocked and incubated with primary antibodies at room temperature for 1 h. After washing, the sections were coincubated with poly-*HRP*-MS/Rb for 10 min at room temperature. All samples were stained with the primary antibody for CD20 (1:100, ab9475, Abcam, UK) visualized with Opal690 TSA, CD3 (1:100, ab135372, Abcam, UK) visualized with Opal480 TSA, CD8 (1:100, ZA-0508, Zsbio, China) visualized with Opal570 TSA, PD-1 (1:100, ZM-0381, Zsbio, China) visualized with Opal520 TSA, FOXP3 (1:100, ab20034, Abcam, UK) visualized with Opal620 TSA. Finally, the sections were covered with an anti-fluorescence attenuating tablet and cover glass.

#### **Immune cell counting, TLS definition, TLS distance analysis and intracellular distance analysis**

**Immune cell counting:** Using StrataQuest 7.1.129 software (TissueGnostics) to identify cell and tissue types and quantify protein expression in panoramic images. Firstly, the software used intelligent algorithms to segment all cells in the tissue area centered around the nucleus, through manual training and machine learning methods for tissue type recognition, tissues can be divided into different regions such as tumors and stroma regions, based on the cytokeratin staining using the Inform Tissue Finder algorithms. Then, individual cells were segmented using the counterstain-based cell segmentation algorithm, based on DAPI staining. Quantification of the specific immune cells was performed using the Inform scoring tool by assigning a threshold to the different cell phenotypes, based on the staining intensity of each marker. The protein expression quantification was performed by determining the average fluorescence threshold of each detected marker, in order to determine the number of positive cells labeled by that marker, positive cells are defined as those that have detected immunofluorescence signals greater than the threshold and have the correct expression pattern. Cell density (cells/ $\text{mm}^2$ ) for CD8+cells, CD3+cells, FOXP3+cells, CD20+cells, PD-1+CD3+cells, PD-1+CD8+cells, PD-1+FOXP3+cells, PD-1+CD20+cells was quantified in whole tumor sections and TLS areas by the StrataQuest 7.1.129 software (TissueGnostics) [38].

**TLS definition:** For TLS definition and quantification, the stained slides were panoramic scanned and visualized using the the Tissue FAXS (SL 7.1.120). Multicolor fluorescence images were analyzed with StrataQuest 7.1.129 software (TissueGnostics). Structures were identified as aggregates of lymphocytes having histological features with analogous structures to that of lymphoid tissue

with B cells (CD20), T cells (CD3/CD8). The aggregation degree was identified to screen for areas that might be TLS, and then it was manually confirmed by HE stained images. TLS counting was defined as the total number of structures identified either within the tumoral area or in direct contact with the tumoral cells on the margin of the tumors [39].

**TLS distance analysis:** After TLSs were filtered out, the distance between TLSs and the closest tumor cells was measured using the distance measurement. **Intracellular distance:** We found the nearest cell by using one of the cells as a fixed point based on the coordinate axis position, and then we calculated the distance between them. All the analyses mentioned above were conducted by StrataQuest 7.1.129 software (TissueGnostics) [40].

#### **Flow cytometry**

Fresh tumor samples were collected after the surgery. All tissue samples were cut into tiny pieces and incubated in DMEM (Cat# 11054001, Gibco) containing 10% FBS (200 U/ml), type IV collagenase (Cat# C5138, Sigma) for 35 min at 37 °C on a shaker (200 rpm). Then the dissociated cell suspensions were filtered through 70  $\mu\text{m}$  cell strainers and 40  $\mu\text{m}$  cell strainers (Cat# 352340 and Cat# 352360, Falcon) to obtain single-cell suspensions. PBMCs were isolated by density gradient centrifugation (speed at 2000 rpm; acceleration ramp 3 and braking ramp 0) for 20 min using Ficoll-Paque Plus (Cat# 17-1440-03-1, GE Healthcare). Single-cell suspensions were prepared as described above. The cells were collected and transferred to flow tubes. Single cells were stained with different antibodies (antibody information was shown in) in PBS containing 2% FBS for 30 min at 4 °C in the dark place. Cells were then fixed and permeabilized with fixation/permeabilization concentrate (Cat#00-5123-43, eBioscience) for 35 min at room temperature in dark place. Intracellular targets were stained with corresponding antibodies for 35 min at room temperature, followed by two wash steps with permeabilization buffer (Cat# 00-8333-56, eBioscience). A BD LSRFortessa X-20 cell analyzer were used for flow cytometry analysis. Data analysis was performed with FlowJo v10 (FlowJo LLC). The following flow cytometry antibodies were purchased from BD Horizon™: CD3 (SP34-2), CD8 (SK1), FOXP3 (259D/C7), CD25 (M-A251), PD-1 (EH12.1).

#### **RNA sequencing**

Bulk RNA derived from biopsy fresh tumor tissue samples was extracted using RNeasy Plus Mini Kit (74134, QIAGEN, Germany) according to the manufacturer's instructions. Raw sequencing reads were pre-processed using fastp v0.12.6. with default parameters and additional trimming of the first 10 bases of the reads for subsequent analysis. After quality control, clean data were



aligned to the reference genome (GRCh37) with STAR (version 2.7.8a). FeatureCounts was used to estimate the expression level of each gene. Gene expression was quantified as transcripts per million (TPM). We used the DESeq2 package of R software (4.2.0) to screen differentially expressed genes between comparisons, with the following threshold:  $|\log_2(\text{Fold Change})| > 1$  and  $p \text{ value} < 0.05$ . Paired regression analysis using DESeq2 was performed to identify differentially expressed genes (DEGs) associated with histologically paired lesions. Gene set variation analysis (GSVA). (<https://www.biocconductor.org/packages/release/bioc/html/GSVA.html>) of whole gene sets was conducted using the canonical Broad C2 collection of gene sets in the molecular signature database (MsigDB) based on the expression data.

#### Gene ONTOLOGY analysis

Gene Ontology analysis was performed using Metascape software, which was available online (<http://metascape.org>). Genes were uploaded to the website, and the expression analysis option was selected.

#### ssGSEA

Single-sample Gene Set Enrichment Analysis (ssGSEA) with the GSVA function in R (version 1.42.0) was used to estimate the abundance of specific cell subsets in the tumor microenvironment. This method enabled us to infer the abundance of 28 cell subsets in each sample based on their expression data.

#### Co-expression

Co-expression method for 14 types of immune cells exerted significant differences in the abundance of various immune cell subsets between the experimental group and the control group [41].

#### CYT

Further investigation of the immune characteristics associated with CYT (Cytolytic Activity) revealed that CYT calculates genes per million transcripts using the log average (geometric mean) of GZMA and PRF1 to determine the effect of T cells on tumor cells. There was significant difference in killing energy between groups.

The calculation formula was as follows [42]:

$$C_{YT} = \frac{GZMA \log_2(TPM + 1) + PRF1 \log_2(TPM + 1)}{2}$$

#### Xcell

XCell algorithm based on R package xCell master was used to infer 64 types of immune and stromal cells in the sample [43].

#### GEP

Immune sensitive features GEP (18 genes in T cell-inflamed gene expression profile) score. GEP immune signature can be classified into the following three categories:

- 1) (1) 10-Gene preliminary IFN -  $\gamma$  signature: includes.
- 2) IFNG, STAT1, CCR5, CXCL9, CXCL10, CXCL11, IDO1, PRF1, GZMA, and MHCII HLA-DRA;
- 3) (2) Expand 28 gene set IFN- $\gamma$  signature: including cytolytic activity, cytokines/chemokines, T cell markers, NK cell activity, antigen presentation, and additional immunomodulatory factors;
- 4) (3) T cell-inflamed GEP: including CXCR6, TIGIT, CD27, CD274, PDCD1 LG2, LAG3, NKG7, PSMB10, CMKLR1, CD8A, IDO1, CCL5, CXCL9, HLA. DQA1, CD276, HLA.DRB1, STAT1, HLA.E.

The calculation formula is as follows [44]:

$$T \text{ cell inflamed GEP Score} = \text{the weighted sum of the housekeeping normalized values of the 18 genes}$$

#### TLS signature

TLS signature referred to the signature related to the tertiary lymphatic structure [45].

#### Statistical analysis

Tumor infiltrating lymphocyte (TIL) levels between pre- and post-treatment biopsy specimens were compared using paired t tests. Univariate and multivariate analyses were performed by using a logistic regression model. Variables that substantiated statistical significance in the univariate analysis were included in the multivariate analysis. Survival was calculated using the Kaplan–Meier method and compared using the log-rank test. Multivariable-adjusted Cox proportional hazards regression was performed to analyze response and survival after treatment. Differences in survival curves between groups were compared using the Log-Rank test, and statistical significance was set at  $P \text{-values} < 0.05$ . The odds ratio (OR) was reported with a 95% CI. Best cut-off were determined by using the receiver operating characteristics (ROC) curve analysis, and the best cut-off was the one that maximized the area under the curve (AUC). Statistical analysis was performed using SPSS software (SPSS Statistics, version 26); GraphPad Prism 9.0.0 software was applied in the multiplex immunohistochemistry staining result interpretation and Forest plot. The Chi-Square Test was used to compare rates in independent groups. All statistical tests were two-sided and  $P \text{-values} < 0.05$  were considered statistically significant.

## Results

### Baseline characteristics of 68 gastric cancer patients

The study flowchart was presented in Fig. 1. Firstly, 68 patients who underwent gastrectomy between May 2017 and December 2021 were collected for analysis (Table S1). To better exclude the influence of chemotherapy and distinguish between Stage I early gastric cancer and advanced gastric cancer, we excluded cases received chemotherapy in Stage I patients. With regard to patients with advanced gastric cancers, we selected the cases only received conventional chemotherapy to exclude the influence of postoperative immunotherapy. 68 samples including 49 males and 19 females surgically resected gastric cancer. The median overall survival time is 37.2 months (range:2–84 months), and the median age at diagnosis is 65 years (range:24–81 years). The tissue pathological type consist of 5 cases of papillary adenocarcinoma (pap), 16 cases of tubular adenocarcinoma (tub), 31 cases of poor-differentiated adenocarcinoma (por), 5 cases of mucinous adenocarcinoma (muc) or signet ring cell (sig) type (pathological classification by Japanese Classification). To sum up, 17 GC lesions occurred in “the upper parts of the stomach”, 18 GC tumors occurred in “the middle parts of the stomach”, and 33 GC cases occurred in “the lower parts of the stomach”. The tumors were classified based on clinical TNM Stages, including 13 cases of Stage I, 55 cases of Stage II-IV (Table S1).

### PD-1+Treg/PD-1+CD8>1 could be regarded as an independent predictor of prognosis in advanced gastric cancer patients

For the flow cytometry analysis of fresh tumor samples from 68 gastric cancer patients, PD-1+Treg infiltration was high in Stage I patients, and with the progression of the disease, the infiltration of PD-1+Treg slashed. Accordingly, the infiltration of PD-1+CD8+T cells did not change significantly with the progression of the disease (Fig.S1, S2A, B). In addition, we found that the ratio of PD-1+Treg/PD-1+CD8 ranks the highest in Stage I, with the progression of the disease, the ratio plunged. Specifically, patients with high PD-1+Treg/PD-1+CD8 ratio had a significant high rate in Stage I than those in Stage II-IV ( $p<0.001$ ). The same trend was also been observed in the PD-1+Treg/ PD-1+CD4 ratio ( $p=0.006$ ). Moreover, PD-1+Treg/PD-1+CD8>1 could be an independent doomy prognostic factor in the Stage II-IV group in the multivariable survival analysis (HR: 2.689, 95% CI 1.138–5.489,  $p=0.007$ ) (Fig. 2A, B,C; Table 1). Nevertheless, the corresponding trend was not reflected in the peripheral blood samples of patients (data was not shown). Through multivariable-adjusted cox proportional hazards regression, we found that pathological type, location, and PD-1+Treg/PD-1+CD8>1 were independent predictors in advanced gastric cancer patients (Fig. 2D).

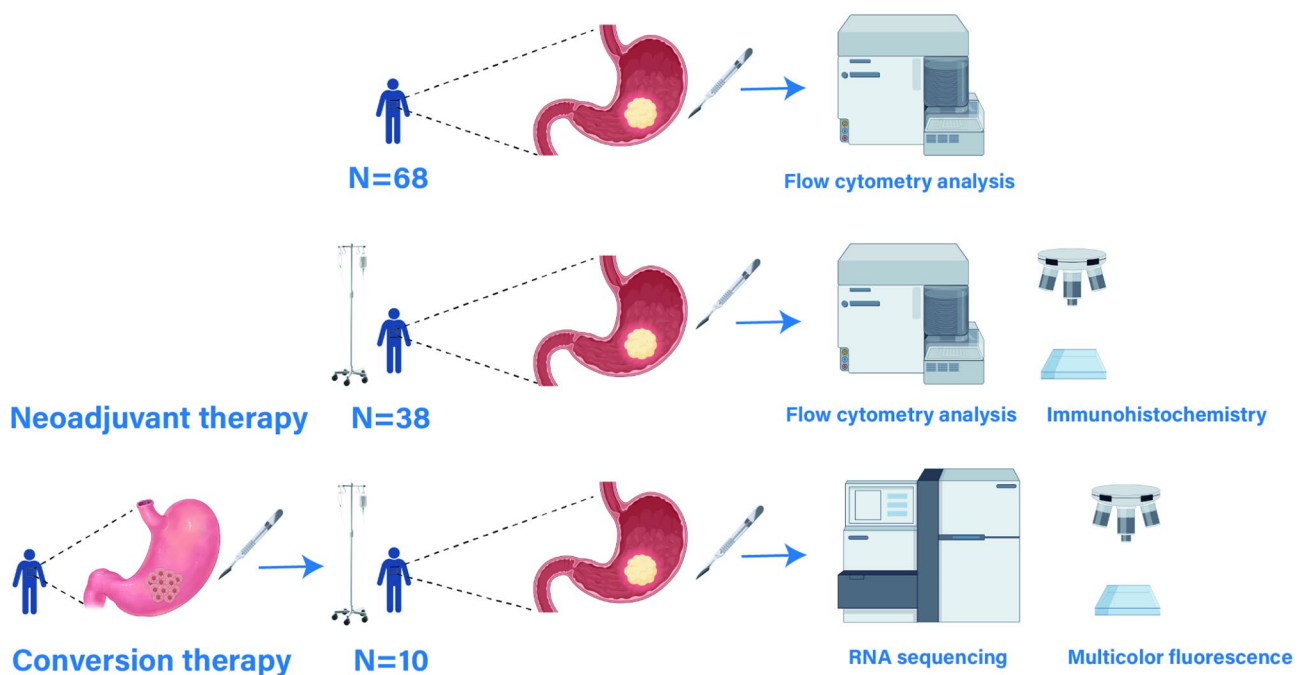


**Fig. 1** Study flowchart for the analysis

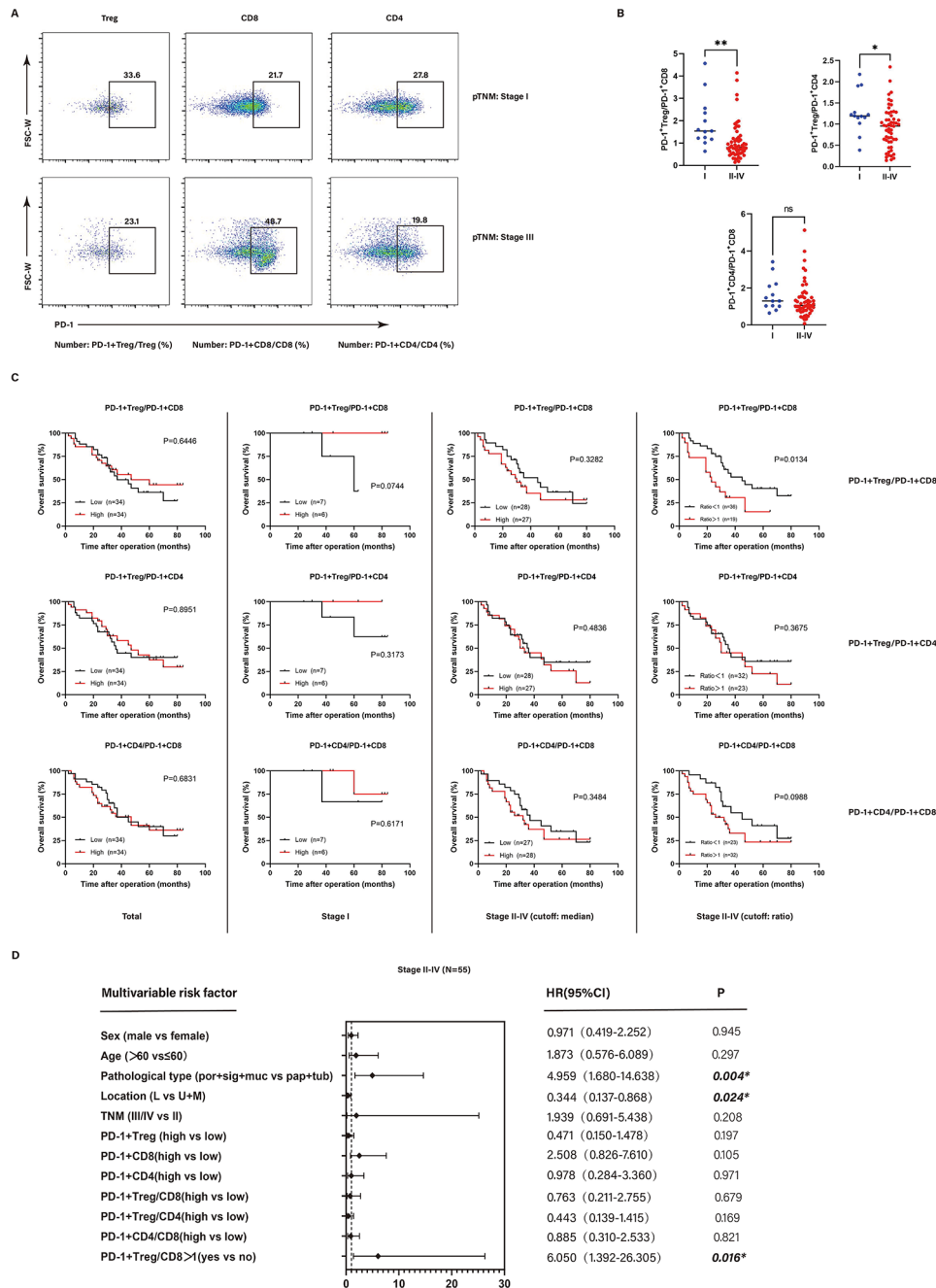


**Fig. 2** The correlation between T cell ratios and prognosis of gastric cancer patients at different stages. **(A)**: Representative images of the proportion of PD-1+Treg, PD-1+CD8, PD-1+CD4 in Stage I and Stage III gastric cancer; **(B)**: The proportion of PD-1+Treg/PD-1+CD8, PD-1+Treg/PD-1+CD4, PD-1+CD4/PD-1+CD8 between Stage I and Stage II-IV gastric cancer; **(C)**: The Correlation of PD-1+Treg/PD-1+CD8, PD-1+Treg/PD-1+CD4, PD-1+CD4/PD-1+CD8 with GC patients' overall survival. Kaplan–Meier survival curves for OS based on PD-1+Treg/PD-1+CD8, PD-1+Treg/PD-1+CD4, PD-1+CD4/PD-1+CD8 in total GC patients in Stage I and Stage II-IV GC patients (cutoff values are ratios>1 and median, respectively.); **(D)**: Forest plot displaying the multivariate regression analysis of risk factors affecting 55 advanced GC. (\* and \*\* represented P-values less than 0.05 and 0.01, respectively. ns: no statistical significance)

**PD-1+Treg/PD-1+CD8 < 1 and high expression of TLS could indicate better neoadjuvant therapy response and extended survival time in advanced gastric cancer patients**  
 Due to the discovery of the predictive value of PD-1+Treg/PD-1+CD8 ratio for the prognosis of

gastric cancer patients, we further discussed the impact of PD-1+Treg/PD-1+CD8 ratio and other immune factors on treatment response in advanced gastric cancer. By analyzing the flow cytometry data and results of immunohistochemistry staining of 38 gastric cancer patients who

**Table 1** Univariate analysis and multivariate analysis for total and subgroup in 68 GC patients

Risk factors	Univariate analysis			Multivariate analysis		
	HR(95%CI)		P	HR(95%CI)		P
<b>Total</b>						
Age	1.045	(1.007–1.085)	<b>0.021*</b>	1.045	(1.004–1.087)	<b>0.031*</b>
Gender: male	1.12	(0.539–2.327)	0.761			
Pathological type	1.445	(0.958–2.181)	0.079			
Location	0.763	(0.519–1.122)	0.169			
Advanced vs. early	6.394	(1.529–26.734)	<b>0.011*</b>	5.926	(1.415–24.825)	<b>0.015*</b>
PD-1 + Treg: high	1.327	(0.685–2.571)	0.402			
PD-1 + CD8:high	1.574	(0.807–3.071)	0.184			
PD-1 + CD4:high	1.688	(0.868–3.283)	0.123			
PD-1 + Treg/CD8:high	0.935	(0.480–1.820)	0.842			
PD-1 + Treg/CD8>1	1.223	(0.612–2.445)	0.568			
PD-1 + Treg/CD4:high	0.905	(0.485–1.690)	0.754			
PD-1 + CD4/CD8:high	1.226	(0.663–2.266)	0.515			
<b>Stage I</b>						
Age	1.094	(0.878–1.362)	0.423			
Gender: male	0.378	(0.023–6.209)	0.496			
Pathological type	0.207	(0.019–2.282)	0.199			
Location	68.67	(0.024–193543.017)	0.297			
PD-1 + Treg: high	1.581	(0.097–25.767)	0.748			
PD-1 + CD8:high	2	(0.125–31.975)	0.624			
PD-1 + CD4:high	59.152	(0.001–5329486.111)	0.483			
PD-1 + Treg/CD8:high	0.008	(0.000–1357.465)	0.435			
PD-1 + Treg/CD8>1	0.742	(0.168–3.272)	0.693			
PD-1 + Treg/CD4:high	0.471	(0.018–12.043)	0.649			
PD-1 + CD4/CD8:high	0.5	(0.031–7.994)	0.624			
<b>Stage II-IV</b>						
Age	1.039	(0.998–1.083)	0.064			
Gender: male	1.21	(0.564–2.597)	0.625			
Pathological type	1.575	(0.970–2.557)	0.066			
Location	0.673	(0.461–0.981)	<b>0.040*</b>	0.681	(0.461–1.006)	0.054
TNM stage	2.336	(1.065–5.120)	<b>0.034*</b>	2.713	(1.191–6.182)	0.018
PD-1 + Treg: high	1.441	(0.724–2.865)	0.298			
PD-1 + CD8:high	1.458	(0.729–2.914)	0.286			
PD-1 + CD4:high	1.353	(0.687–2.663)	0.382			
PD-1 + Treg/CD8:high	1.501	(0.751–2.960)	0.242			
PD-1 + Treg/CD8>1	2.576	(1.281–5.178)	<b>0.008*</b>	2.689	(1.318–5.489)	<b>0.007*</b>
PD-1 + Treg/CD4:high	1.082	(0.551–2.124)	0.819			
PD-1 + CD4/CD8:high	1.48	(0.750–2.918)	0.258			

\*p-value&lt;0.05

underwent neoadjuvant immunotherapy and chemotherapy (including 21 responders and 17 non-responders), we observed a significant increase in PD-1+CD8+T cells along with high expression of TLS in patients with better neoadjuvant therapy response (Fig. 3A, B, C). We found that only the combination of PD-1+Treg/PD-1+CD8<1 and TLS has a significant correlation with the response group through statistical analysis ( $p=0.018$ ). (Table 2).

Regarding the PD-1+Treg/PD-1+CD8 ratio for predicting response status, the area under the curve (AUC) by ROC analysis was 0.809. The optimal cut-off by the Youden index was 0.1457, resulting in the sensitivity of

85.7% and specificity of 70.6% (Fig. S3A). However, considering its clinical feasibility, we still used the ratio<1 as a criteria in the following analysis. Subsequently, we conducted ROC curves for PD-1+Treg/PD-1+CD8<1 and TLS high expression, as well as their combined indicators, discovering that only the combined group had statistical significance in predicting response ( $p=0.0443$ ) (Fig. S3B). Then we conducted survival analysis in the 38 gastric cancer patients mentioned above. Intriguingly, we found that patients with PD-1+Treg/PD-1+CD8<1 and high TLS expression had significantly prolonged survival ( $p=0.0334$ ), which was also a statistically significant



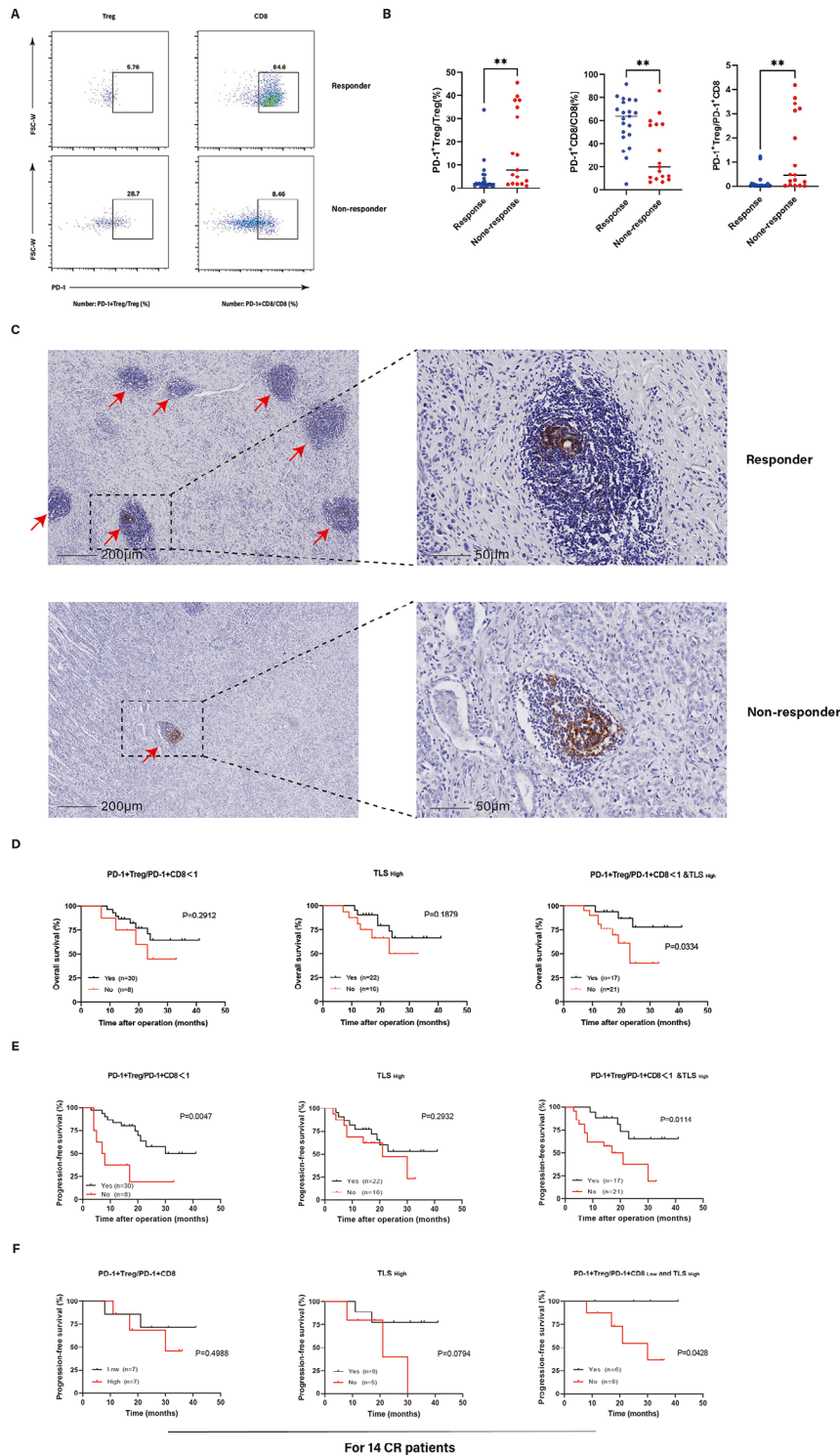


**Fig. 3** The correlation of PD-1 + Treg/PD-1 + CD8 ratio & TLS and neoadjuvant response as well as survival in advanced gastric cancer patients. **(A)**: Representative images of the proportion of PD-1 + Treg, PD-1 + CD8 in responders and non-responders; **(B)**: The proportion of PD-1 + Treg, PD-1 + CD8, PD-1 + Treg/PD-1 + CD8 in responders and non-responders; **(C)**: The tertiary lymphoid structures expression in gastric cancer by immunohistochemistry staining (x5). The representative images of responders and non-responders. (The right panel: x20). **(D)**: The Correlation of PD-1 + Treg/PD-1 + CD8, TLS, PD-1 + Treg/PD-1 + CD8<sub>low</sub> and TLS<sub>high</sub> with GC patients' overall survival; **(E)**: The Correlation of PD-1 + Treg/PD-1 + CD8, TLS, PD-1 + Treg/PD-1 + CD8<sub>low</sub> and TLS<sub>high</sub> with GC patients' progression-free survival; **(F)**: The Correlation of PD-1 + Treg/PD-1 + CD8, TLS, PD-1 + Treg/PD-1 + CD8<sub>low</sub> and TLS<sub>high</sub> with 14 CR patients' progression-free survival. (\*, \*\*, and \*\*\* represent P-values less than 0.05, 0.01, and 0.001, respectively. ns: no statistical significance)

**Table 2** Clinicopathological factors of included 38 neoadjuvant therapy AGC patients

	PD-1 + Treg/PD-1 + CD8<1				TLS: High				PD-1 + Treg/PD-1 + CD8<1 and TLS: High			
	n	No(%)	Yes(%)	p-value	No(%)	Yes(%)	p-value	No(%)	Yes(%)	p-value		
<b>Gender</b>	38			0.248			0.321			0.508		
Female	11	9.1	90.9		54.6	45.4		63.6	36.4			
Male	27	25.9	74.1		37	63		51.9	48.1			
<b>Age</b>	38			0.867			0.299			0.203		
≤60	20	20	80		50	50		65	35			
>60	18	22.2	77.8		33.3	66.7		44.5	55.5			
<b>Location</b>	38			0.367			0.343			0.524		
U	14	21.4	78.6		57.1	42.9		64.3	35.7			
M	16	12.5	87.5		31.2	68.8		43.7	56.3			
L	8	37.5	62.5		37.5	62.5		50	50			
<b>Pathological classification</b>	38			0.485			0.403			0.454		
Pap	7	0	100		42.9	57.1		42.9	57.1			
Tub	10	30	70		20	80		40	60			
Poor	17	23.5	76.5		52.9	47.1		64.7	35.3			
Sig+Muc	4	25	75		50	50		75	25			
<b>yPTNM</b>	38			0.931			0.671			0.653		
1	15	20	80		33.3	66.7		46.7	53.3			
2	6	16.7	83.3		50	50		66.7	33.3			
3	17	23.5	76.5		47.1	52.9		55.8	44.2			
<b>Response</b>	38			0.053			0.060			<b>0.018*</b>		
Yes	21	9.5	90.5		28.6	71.4		38.1	61.9			
No	17	35.3	64.7		58.8	41.2		76.5	23.5			

U: upper parts; M: middle parts; L: lower parts. Pap: papillary adenocarcinoma; Tub: tubular adenocarcinoma; Por: poor-differentiated adenocarcinoma; Sig: signet ring cell adenocarcinoma; Muc: mucinous adenocarcinoma  
\*p-value < 0.05

factor in univariate analysis along with ypTNM stage and response (Table 3). Also, we found that both PD-1+Treg/PD-1+CD8<1 and combined indicators could distinguish PFS with significant differences, while only the combined indicator was considered an independent predictor of PFS in multivariable-adjusted cox proportional hazards regression analysis ( $p=0.039$ ) (Fig. 3D, E, Table S2, S3). Owing to a dearth of samples before neoadjuvant therapy, we were regrettably unable to predict the response of patients after treatment. Actually, in clinical practice, even a subset of CR cases relapsed without postoperative treatment [46]. This is why surveillance and additional treatment is crucial to certain patients who have achieved CR currently. Consequently, we were dedicated to the 14 CR patients in the response group (all of them did not receive postoperative adjuvant chemotherapy). In this section, due to the fact that almost all patients in this subgroup had the characteristic of PD-1+Treg/PD-1+CD8 ratio<1, patients were dichotomized into the high- and low- group according to the median of PD-1+Treg/PD-1+CD8 ratio. Intriguingly, the PFS of the PD-1+Treg/PD-1+CD8<sub>low</sub> and TLS<sub>high</sub> group was significantly prolonged, which may guide the postoperative treatment of certain CR patients to some extent ( $p=0.0428$ ) (Fig. 3F).

#### PD-1 + CD8 + T cells infiltration raised, accompanied by an increase in TLS after treatment

Meanwhile, 10 pairs of cases using preoperative immunotherapy plus chemotherapy with complete preoperative laparoscopic biopsy specimens and postoperative surgical specimens were selected for further exploration. To begin with, we compared the differences in immune cell infiltration before and after conversion therapy using multi-color fluorescence staining (Fig. S4A, B, C). It was found that CD8+T cell density in tumor increased significantly after treatment. Next, as for cell subpopulations, we found that PD-1+CD8+T cell density in tumor multiplied after conversion therapy (Fig. S5A, B), though, there was no significant difference in the various cell subsets of

stroma after treatment (data was not shown). Meanwhile, the number of TLS slightly increased after treatment among all cases, but there was no statistical significance (Fig. S5C).

Based on RECIST 1.1 and postoperative pathological TRG, we defined a response group of 5 cases and a non-response group of 5 cases to conversion therapy (Fig. 4A, B). In response group, PD-1+CD8+T cells increased after treatment, accompanied by the rise of TLS expression (Fig. 4C, D, E). By contrast, in non-responsive group, no similar trend was observed (data not shown). Through univariate analysis of 10 gastric cancer patients who underwent conversion therapy, due to the limited sample size, the post-treatment PD-1+Treg/PD-1+CD8 ratio and TLS combination group was considered a protective factor, but it did not show statistical significance (HR: 0.013, 95% CI 0.000–161.723,  $p=0.366$ ) (Table S4).

#### PD-1 + CD8 + T cells infiltration increased mainly outside of TLS after treatment

Next, we conducted statistical analysis on the subsets of cells inside and outside the TLS based on multi-color immunofluorescence results. We found that among CD3+, CD8+, FOXP3+, CD20+, and PD-1+subsets, only CD20+cells exerted a significant increase within TLS compared to the outside after treatment with significant statistical differences (Fig. 5A, B, C). When we analyzed the TLS/nTLS (non-TLS areas) ratio before and after treatment, we found that the TLS/nTLS ratio of CD20+cells, PD-1+CD3+cells, and PD-1+CD20+cells significantly increased after treatment, while the TLS/nTLS ratio of PD-1+CD8+cells decreased (Fig. 5D). To some extent, this phenomenon indicated that the increment in PD-1+CD8+cells after treatment mainly infiltrating outside of TLS, which was opposite to PD-1+CD20+cells.

Subsequently, in the analysis of the average distance between TLS and the nearest tumor area, there was a trend of shorter distance observed in the response group after treatment, but the results were not statistically

**Table 3** Univariate analysis and multivariate analysis for 38 neoadjuvant therapy AGC patients

Risk factors	Univariate analysis		Multivariate analysis		
	HR(95%CI)	P	HR(95%CI)	P	P
Age	0.965	(0.923–1.010)	0.126		
Gender: male	0.797	(0.216–2.945)	0.797		
Pathological Type: Sig + Muc + Por	1.129	(0.358–3.563)	0.836		
Location: L	1.055	(0.284–3.928)	0.936		
ypTNM: III	3.372	(1.008–11.283)	<b>0.049*</b>	2.270	(0.637–8.083)
Response: Yes	0.143	(0.037–0.553)	<b>0.005*</b>	0.237	(0.039–1.435)
PD-1 + Treg/CD8<1	0.533	(0.160–1.774)	0.305		
TLS: High	2.117	(0.669–6.701)	0.202		
PD-1 + Treg/CD8<1 TLS: High	0.264	(0.070–0.994)	<b>0.049*</b>	0.637	(0.116–3.511)

\*p-value<0.05

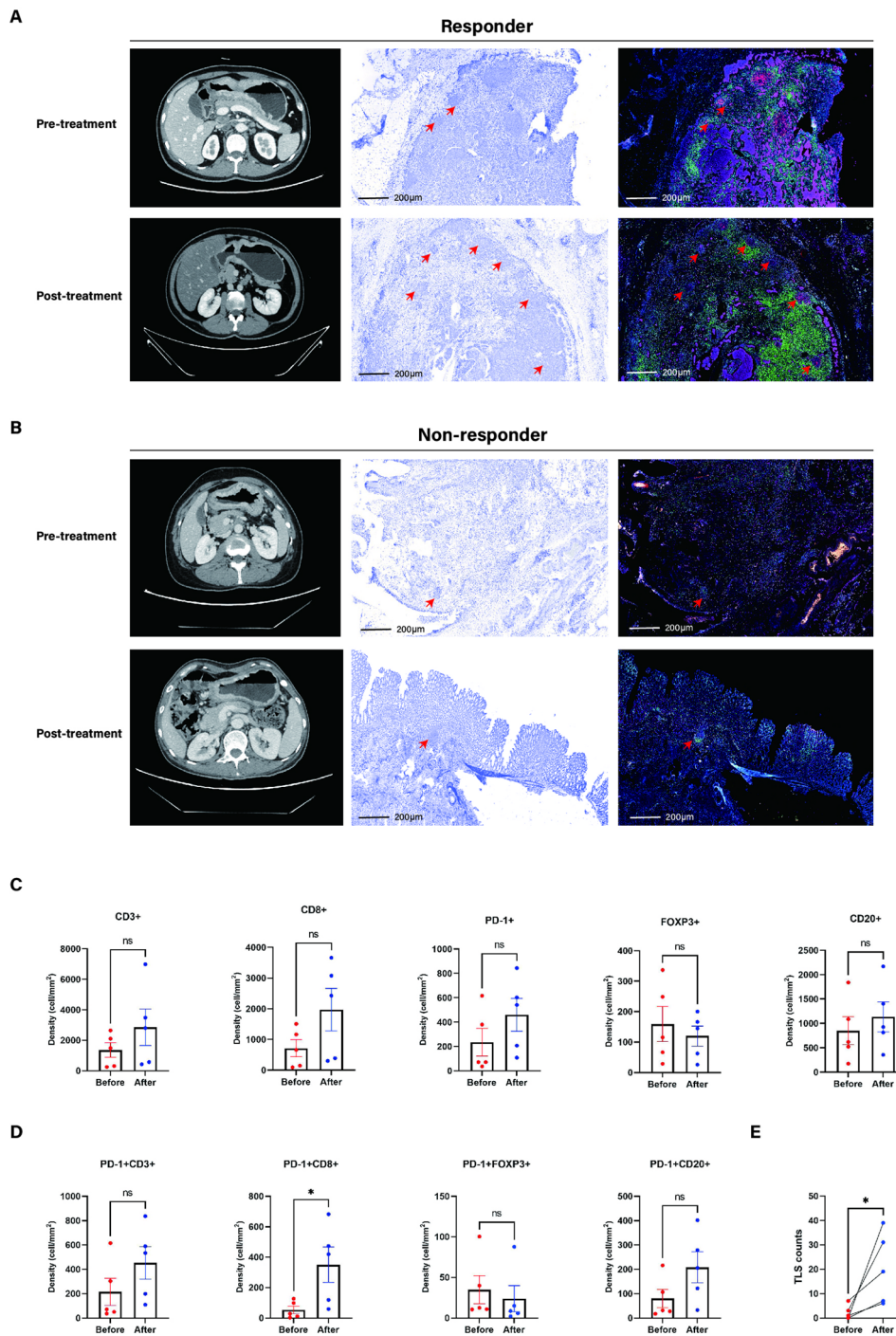


**Fig. 4** Representative CT images and fluorescence images between responders and non-responders. **(A)**: Representative CT images and fluorescence images of responders before and after conversion treatment; **(B)**: Representative CT images and fluorescence images of non-responders before and after conversion treatment (The red arrows indicate TLS); **(C)**: The density of CD3+, CD8+, PD-1+, FOXP3+ and CD20+ cells between pre- and post-conversion therapy in responders; **(D)**: The density of PD-1 + CD3+, PD-1 + CD8+, PD-1 + FOXP3+ and PD-1 + CD20+ cells between pre- and post-conversion therapy in responders; **(E)**: The TLS counts between pre- and post-conversion therapy in responders. (\*represented P-values less than 0.05, respectively. ns: no statistical significance)



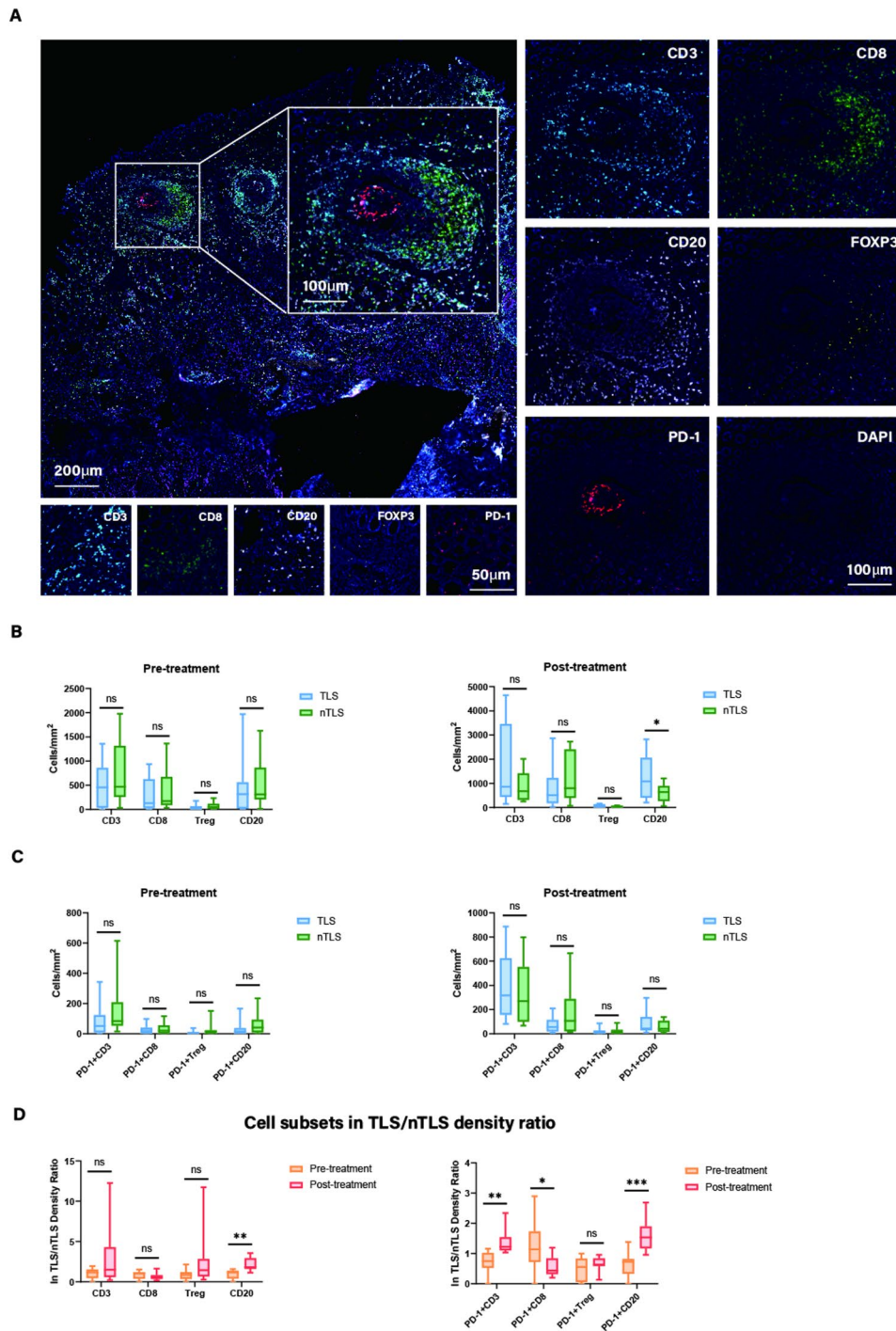


**Fig. 5** Distribution of immune cell subsets inside and outside TLS. **(A)**: Characteristics of immune cell subsets inside TLS by multicolor immunofluorescence staining; **(B)**: The density of CD3、CD8、Treg and CD20 between TLS and nTLS before and after treatment. **(C)**: The density of PD-1+CD3、PD-1+CD8、PD-1+Treg and PD-1+CD20 between TLS and nTLS before and after treatment. **(D)**: Cell subsets in TLS/nTLS density ratio before and after treatment. (\*, \*\*and\*\*\* represented P-values less than 0.05, 0.01 and 0.001, respectively. ns: no statistical significance)

significant (Fig.S6A, B). Then, in the analysis of the average intracellular distance before and after treatment, we found that the distances between PD-1+cells and CD8+cells, PD-1+cells and CD20+cells, CD3+cells and CD20+cells were significantly shortened, which further

confirmed our former conclusions that there existed an increase in PD-1+CD8+T cells infiltration accompanied by increment of TLS after treatment to some extent (Fig.S6C).

### Transcriptome analysis of tumors before and after conversion therapy

For these 10 pairs of samples before and after conversion therapy, we conducted transcriptome sequencing analysis. Regarding the analysis of differences before and after conversion therapy, GO analysis demonstrated a significant correlation with the “collagen-containing extracellular matrix”, “guanyl-nucleotide exchange factor activity”, and “muscle system process” (Fig.S7A, B,C). Pathway signature analysis related to KEGG metabolism exerted the significant difference about “Glycosaminoglycan degradation” and “Purine metabolism”(Fig.S7D). In terms

of immune analysis, post-treatment group presented more immunocostimulators (Fig. 6A). The analysis of the abundance of 14 immune cell populations using Co-expression indicated significant differences in the abundance of mast cell between the post-treatment group and the prior-treatment group (Fig. 6B). Moreover, quantitative analysis of 28 immune cellular subpopulations in the tumor microenvironment was conducted by using ssGSEA method. A comparative analysis of the infiltration of 28 immune cells displayed a significant increase in activated-CD8+T cell infiltration in the post-treatment group (Fig. 6C). Besides, we investigated the immune

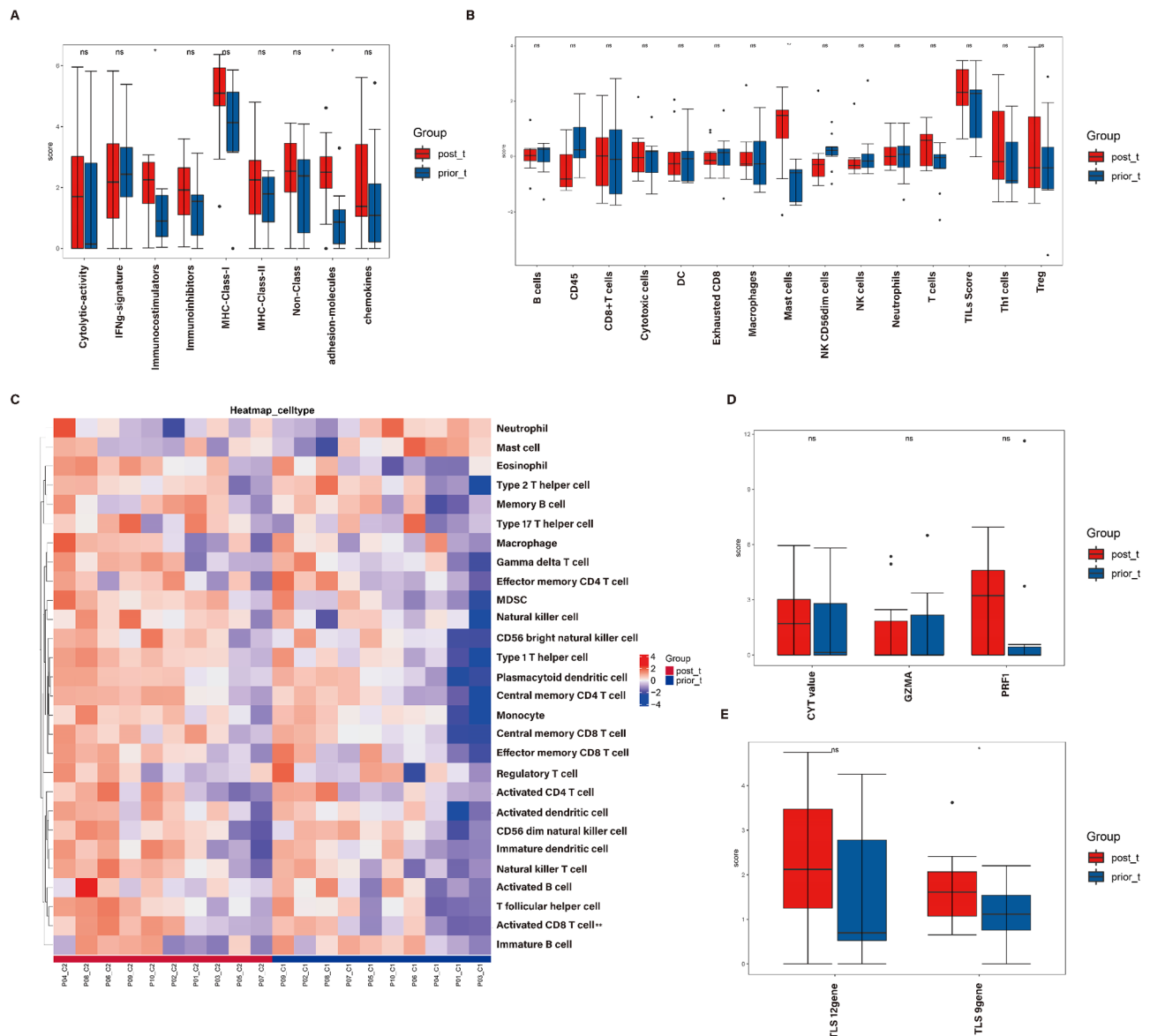


**Fig. 6** Related immune analysis between prior- and post-conversion therapy. **(A)**: The Box diagram of immunoactivity analysis; **(B)**: Abundance boxplot of immune cell subsets between groups; **(C)**: Heat map of infiltration analysis of immune cell subsets between groups; **(D)**: Boxplot of T cells' ability to kill tumor cells between groups; **(E)**: Box map of tertiary lymphoid structure correlation features. (\* and \*\* represented P-values less than 0.05 and 0.01, respectively. ns: no statistical significance)

characteristics related to CYT (Cytolytic activity) analysis. There was no statistically significant difference in killing energy between prior- and post-groups (Fig. 6D). Obviously, TLS-signature referred to the signature which was related to the tertiary lymphatic structure. Similar to the above research trends, sequencing results suggested that the TLS 9 genes signature was significantly upregulated after treatment (Fig. 6E). Furthermore, to describe the characteristics of tumor cells, inter-group functional state analysis was conducted. It implied that the apoptosis and hypoxia may have significant changes after treatment (Fig.S8A). However, the GEP (18 genes in T cell-inflamed gene expression profile) comparison analysis of immune sensitive features indicated no significant difference (Fig.S8B). With the goal of further refining the features of the immune microenvironment, the xCell algorithm based on R package xCell master was applied. It inferred that “chondrocytes”, “epithelial cells”, “HSC”, “Th2 cells” and “cDC” were significantly altered after treatment (Fig.S8C).

## Discussion

There have been huge amounts of studies discussing the relationship between cell subsets ratios and disease progression in the tumor immune microenvironment. Among them, the effects of CD4/CD8, CD8/Treg, as well as PD-1+CD8/PD-1+CD4 ratios on post-treatment response have been extensively reported [47–49]. However, as a balancing factor to play a decisive role in PD-1 therapy, PD-1+Treg/PD-1+CD8 ratios in gastric cancer has not been systematically discussed yet.

In this research, we concentrated on exploring the association of PD-1+Treg/PD-1+CD8 ratios with prognosis and treatment response in gastric cancer. In 68 fresh gastric cancer samples, the PD-1+Treg/PD-1+CD8 ratio in advanced gastric cancer was found to exert an inverted trend compared to early gastric cancer for the first time. In advanced gastric cancer, PD-1+Treg/PD-1+CD8 ratio>1 could be an independent doomy prognostic factor, which is a thought-provoking phenomenon. To our knowledge, this is the first relative large-scale flow cytometry data from fresh tumor sample of gastric cancer with high reliability. In theory, patients with a high PD-1+Treg/PD-1+CD8 ratio may experience a proportional imbalance after the application of PD-1 inhibitors, leading to disease progression. Therefore, this population may be considered as an “immune-compromised population”. According to the data of our research, it has been found that the utilization of ICIs in early gastric cancer patients may have the opposite effect, but the “immune-compromised population” still accounts for a considerable proportion in advanced gastric cancer. Therefore, it is of great significance to screen out the “immune

benefiting population” and avoid the “immune-compromised population”.

Afterwards, we directed attention to the immune cell infiltration in advanced gastric cancer patients after neoadjuvant therapy and discovered that the infiltration of PD-1+CD8+T cells in response group significantly increased, indicating a significant drop in the PD-1+Treg/PD-1+CD8 ratio. In addition, by plotting the ROC curve of PD-1+Treg/PD-1+CD8 ratio and response in patients after neoadjuvant therapy, it has been found that this ratio is somewhat related to treatment response.

Given the insights gained from the combined use of TLS and systemic inflammatory markers in a related research [35], we intended to incorporate the concept of tertiary lymphoid structure. Previous studies have indeed suggested that TLS indicated a better response to neoadjuvant therapy in tumors, including gastric cancer [37, 50]. As for the specific mechanisms about how TLS influence the efficacy of neoadjuvant therapies, there were few studies reported on it up to now. In a HER-2(+) gastric cancer cohort, the authors found that patients with lower TLS in the tumor core or lower Tregs had better overall survival in the trastuzumab-exposed group [51]. Luise Rupp et al. claimed that neoadjuvant therapy differentially affected pancreatic ductal adenocarcinoma-infiltrating immune cells and may have detrimental effects on the existing B cell landscape and the formation of TLS [52]. Moreover, another report suggested that the induction of TLS maturation may be a potential mechanism for the effectiveness of neoadjuvant chemoimmunotherapy in resectable non-small cell lung cancer [53].

Considering the current theory of dividing the immune microenvironment into inflamed, excluded or desert immune phenotypes, PD-1+CD8 and TLS may be considered as two “complementary components” in the immune microenvironment [54]. Excitingly, in our research, only the combination of PD-1+Treg/PD-1+CD8<1 and high expression of TLS has a significant correlation with the response group, which can also be considered as independent protective factors in multivariable regression analysis for PFS. Furthermore, we detected the PFS of the PD-1+Treg/PD-1+CD8<sub>low</sub> and TLS<sub>high</sub> group was significantly prolonged in 14 CR patients. Generally, CR patients are not required to receive further treatment after undergoing R0 resection. Based on our research, by combining the PD-1+Treg/PD-1+CD8 ratio and TLS expression, we can further predict and select the population that does not require treatment after operation precisely.

Additionally, we innovatively selected 10 advanced gastric cancer patients who were unable to undergo direct resection at the initial diagnosis. By obtaining tissue sections from their first laparoscopic tumor biopsy and

tumor tissues undergoing surgery after conversion therapy, we performed multiplex immunohistochemistry tests and transcriptome sequencing, aiming to compare the infiltration of immune cells and TLS in the TME before and after conversion therapy. At the same time, including the mutual comparison between the response group and the non-response group, it was also found that the number of TLS in the response group significantly increased after treatment, and the PD-1+Treg/PD-1+CD8 ratio also exerted a significant downward trend. Unfortunately, due to the limited sample size, no correlation between the combination indicators and patient response as well as significant differences in survival curves was observed in these 10 samples. Meanwhile, there were no significant attractive results observed in the comparison of sequencing results between the Response and Non-response groups (data not shown). By analyzing the relationship about immune cell subsets and TLS before and after treatment, we found that the PD-1+CD8+T cells infiltration after treatment was mainly increased outside of TLS. Also, the statistics of the average distance between cells before and after treatment illustrated that the distance between PD-1+cells and CD20+cells, as well as PD-1+cells and CD8+cells, decreased after treatment. Based on the above results, we believed that discussing the combination of PD-1+Treg/PD-1+CD8 ratio

and TLS has certain scientific basis. However, whether the components of TLS would affect the balance of PD-1+Treg/PD-1+CD8 after neoadjuvant therapy, and the specific mechanism by which changes in the proportion of cells in the immune microenvironment contribute to the generation or activation of TLS still require further investigation. In accordance with recent researches, the significance of combined index also needs to be further explored in depth [55, 56]. In a nutshell, the main idea of this research was summarized in the pattern diagram (Fig. 7).

Based on the RNA sequencing results and compared with the prior-treatment group, some genes in the treatment group were significantly upregulated, including PANX1, BMP8A, etc., (data not shown) which have been previously reported to be associated with tumor progression [57, 58]. And GO-BP analysis enriched the changes in related pathways such as muscle contracts, GO-CC analysis suggested changes in exocytic vessel after treatment. As for GO-MF analysis, there was a significant difference in the cyclic nucleotide photosensitive activity. These corresponding alterations after neoadjuvant immunotherapy and chemotherapy are worth further exploration. Moreover, KEGG metabolism related pathways exerted the “Glycosaminoglycan degradation” and

### Advanced gastric cancer tumor microenvironment

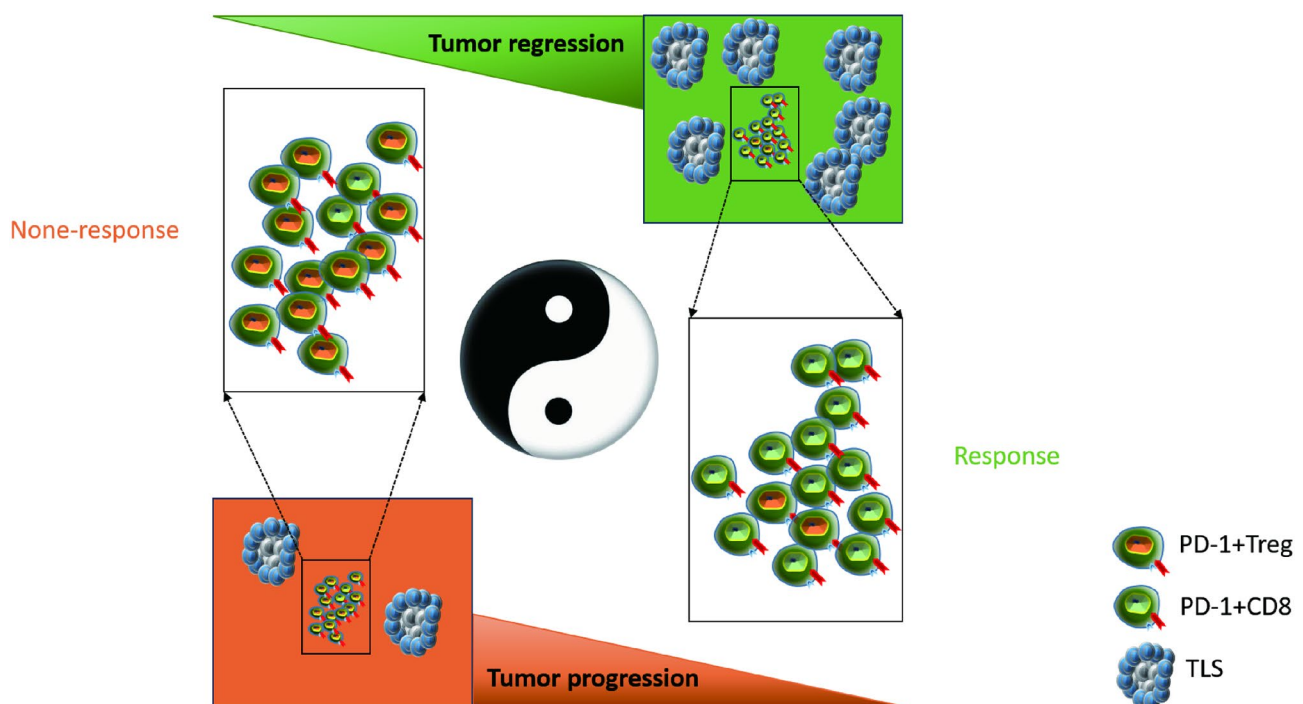


**Fig. 7** The model diagram of immune balance in advanced gastric cancer tumor microenvironment



“Purine metabolism” changed significantly after treatment [59, 60].

With respect to immune analysis, from the perspective of transcriptome and referring to corresponding research, it was combined with the visualization of immune infiltration obtained by multi-color immunofluorescence staining. Firstly, by evaluating the overall immune activity of tumor samples, we found that compared to immune-inhibitors, the scores of immune-costimulators and adhesion-molecules were upregulated, partially indicating the immune activation after treatment. After that, we quantitatively analyzed the infiltration of 28 immune cell subsets in the tumor immune microenvironment. Then, we found that the infiltration of activated CD8+ T cell was significantly upregulated, which was in accord with immunofluorescence results.

However, our study was not without limitations. Firstly, this was a single center retrospective study, and there may exist bias in the selection process of the cohort. Secondly, the number of clinical samples was relatively small, especially the proportion of samples that could be obtained integrally after neoadjuvant therapy and before/after conversion therapy. The limited sample size and potential bias in research design also inevitably caused limitations to this study. More conclusive data in sufficient number of gastric cancer patients cohort with multiple centers and greater diversity are expected to obtain in the future. In addition, through statistical analysis, we found that due to the small sample size, there was no significant difference in immune cell infiltration and TLS distribution between the responsive and non-responsive groups before conversion therapy. This implied that it was not yet possible to prospectively select suitable patients for neoadjuvant or conversion therapy, which was also a barrier that we would focus on tackling in the future. Ultimately, in the study of TLS, we only defined it based on the expression of B and T cells, without subdividing the maturation of TLS.

Thanks to the continuous innovation of advanced technology, precision medicine has been gradually realized. To a certain degree, researches mentioned above were also products of technological innovation. Optimistically, these findings have the opportunity to be further refined and validated by machine learning [61]. As the depth of research on tumor immunology, concepts such as “conventional drug in new use” have also enriched the means of cancer treatment [62, 63]. Moreover, the emergence of nascent biomaterials has provided the possibility for the clinical translation of these research results. For instance, the rapid development of nanomedicine and materials science has provided powerful weapons for tumor immunotherapy [64, 65].

To conclude, further exploration of the microenvironment composition of advanced gastric cancer samples

would have a critical insight into the complex and heterogeneous immune landscape which is associated with tumor progression and neoadjuvant or conversion treatment response. The in-depth exploration of tumor immunology combined with rapidly advancing medical technology has the potential to significantly improve the efficacy of tumor immunotherapy for the benefit of cancer patients.

## Conclusions

This study demonstrated that PD-1+Treg/PD-1+CD8 ratio and TLS were significantly related to prognosis and treatment response in advanced gastric cancer. Patients with low PD-1+Treg/PD-1+CD8 ratio and high TLS score had favorable survival and better preoperative treatment response on the whole. It may provided a new strategy for better predicting the prognosis and treatment responses of advanced gastric cancer patients in the future.

## Abbreviations

AUC	Area under the curve
ROC	Receiver operating characteristics
DEG	Differentially expressed genes
GO	Gene ontology
KEGG	Kyoto Encyclopedia of Genes and Genomes
GSVA	Gene set variation analysis
ssGSEA	Single-sample Gene Set Enrichment Analysis
FFPE	Formalin-fixed, paraffin-embedded
GC	Gastric cancer
HR	Hazard ratio
CI	Confidence interval
ICIs	Immune checkpoint inhibitors
mIHC	Multiplex immunohistochemistry
OS	Overall survival
PFS	Progression-free survival
por	Poor-differentiated adenocarcinoma
pap	Papillary adenocarcinoma
tub	Tubular adenocarcinoma
muc	Mucinous adenocarcinoma
sig	Signet ring cell carcinoma
TLS	Tertiary lymphoid structures
TIL	Tumor infiltrating lymphocyte
Tregs	Regulatory T cells
CR	Complete response
PR	Partial response
PD	Progressive disease
SD	Stable disease
TRG	Tumor regression grading

## Supplementary Information

The online version contains supplementary material available at <https://doi.org/10.1186/s12967-024-05867-4>.

Supplementary Material 1  
 Supplementary Material 2  
 Supplementary Material 3  
 Supplementary Material 4  
 Supplementary Material 5  
 Supplementary Material 6

Supplementary Material 7  
 Supplementary Material 8  
 Supplementary Material 9  
 Supplementary Material 10  
 Supplementary Material 11  
 Supplementary Material 12

### Acknowledgements

We thank all patients who participated in this study and their families. The study flowchart was drawn by Figdraw.

### Author contributions

All authors contributed to the study conception and design. Material preparation, data collection and analysis were performed by Xu Liu, Danhua Xu and Chengbei Zhou. The first draft of the manuscript was written by Xu Liu and all authors commented on previous versions of the manuscript. GC samples were collected by Yiqing Zhong, Haigang Gen, Chen Huang, Xiang Xia, Chaojie Wang. Pathological analysis were evaluated by Yanying Shen. Chunchao Zhu and Hui Cao performed the operation and designed the study. All authors read and approved the final manuscript.

### Funding

This work was supported by the National Natural Science Foundation of China (82203503), National Natural Science Foundation of China (82203224), Chenguang Program of Shanghai Education Development Foundation and Shanghai Municipal Education Commission (22CGA17).

### Data availability

The datasets used and/or analysed during the current study are available from the corresponding author on reasonable request.

### Declarations

#### Ethical approval

All experiments have been approved by the Ethical Committee of the Shanghai Jiao Tong University School of Medicine, Renji Hospital consent from the patient was obtained.

#### Consent for publication

Not applicable.

#### Competing interests

The authors declare that the research was conducted in the absence of any commercial or financial relationships that could be construed as a potential conflict of interest.

#### Author details

<sup>1</sup>Department of Gastrointestinal Surgery, School of Medicine, Renji Hospital, Shanghai Jiao Tong University, 160 Pujian Road, Pudong New Area, Shanghai 200025, China

<sup>2</sup>Division of Gastroenterology and Hepatology, Renji Hospital, School of Medicine, Shanghai Jiao Tong University, 160 Pujian Road, Shanghai 200025, China

<sup>3</sup>Department of Pathology, Renji Hospital, School of Medicine, Shanghai Jiao Tong University, 160 Pujian Road, Shanghai 200025, China

Received: 9 September 2024 / Accepted: 8 November 2024

Published online: 27 December 2024

### References

1. Sung H, Ferlay J, Siegel RL, Laversanne M, Soerjomataram I, Jemal A, et al. Global Cancer statistics 2020: GLOBOCAN estimates of incidence and Mortality Worldwide for 36 cancers in 185 countries. *CA Cancer J Clin.* 2021;71(3):209–49.

2. Li K, Lu S, Leng X, Lin Peng. Comprehensive evaluation of a multicenter real-world study: Neoadjuvant immunochemotherapy in locally advanced gastric cancer. *Int J Surg.* 2024. Online ahead of print.
3. Maeve A, Lowery. Immune-checkpoint blockade in surgical management of gastric or gastro-oesophageal junction adenocarcinoma. *Lancet Gastroenterol Hepatol.* 2024;9(8):679–681
4. Li S, Yu W, Xie F, Luo H, Liu Z, Lv W, et al. Neoadjuvant therapy with immune checkpoint blockade, antiangiogenesis, and chemotherapy for locally advanced gastric cancer. *Nat Commun.* 2023;14(1):8.
5. Kohei Shitara SY, Rha, Lucjan S, Wyrwicz T, Oshima N, Karaseva M, Osipov, et al. Neoadjuvant and adjuvant pembrolizumab plus chemotherapy in locally advanced gastric or gastro-oesophageal cancer (KEYNOTE-585): an interim analysis of the multicentre, double-blind, randomised phase 3 study. *Lancet Oncol.* 2024;25(2):212–24.
6. Mendez SH-BG, Chao J, Nemecek R, Feeney K, Van Cutsem E, et al. First-line nivolumab and Relatlimab Plus Chemotherapy for gastric or gastroesophageal Junction Adenocarcinoma: the phase II RELATIVITY-060 study. *J Clin Oncol.* 2024;42(17):2080–93.
7. Smyth EC, Gambardella V, Cervantes A, Fleitas T. Checkpoint inhibitors for gastroesophageal cancers: dissecting heterogeneity to better understand their role in first-line and adjuvant therapy. *Ann Oncol.* 2021;32(5):590–9.
8. Xiong S, Lyu J, Yang M, Lin Y, Wu K, Liu K, et al. Two-year outcomes and Biomarker Analysis of locally Advanced Gastric and Gastroesophageal Junction Adenocarcinoma after Neoadjuvant Chemotherapy and Immunotherapy from the phase II WuhanUHG1001 trial. *Ann Surg Oncol.* 2024;31(12):8157–69.
9. Wang Z, Cheng S, Yao Y, Liu S, Liu Z, Liu N, et al. Long-term survivals of immune checkpoint inhibitors as neoadjuvant and adjuvant therapy in dMMR/MSI-H colorectal and gastric cancers. *Cancer Immunol Immunother.* 2024;73(9):182.
10. Lorenzo Gervaso D, Ciardiello RA, Oliveira M, Borghesani L, Guidi L, Benini, et al. Immunotherapy in the neoadjuvant treatment of gastrointestinal tumors: is the time ripe? *J Immunother Cancer.* 2024;12(5):e008027.
11. Kohei Shitara M, Özgüroğlu Y-J, Bang MD, Bartolomeo M, Mandalà M-H, Ryu, et al. KEYNOTE-061 investigators. Pembrolizumab versus paclitaxel for previously treated, advanced gastric or gastro-oesophageal junction cancer (KEYNOTE-061): a randomised, open-label, controlled, phase 3 trial. *Lancet.* 2018;392(10142):123–33.
12. Kwon M, An M, Klempner SJ, Lee H, Kim K-M, Jason K, Sa, et al. Determinants of response and intrinsic resistance to PD-1 blockade in microsatellite instability-high gastric Cancer. *Cancer Discov.* 2021;11(9):2168–85.
13. Yibo F, Li Y, Yao X, Jin J, Scott A, Liu B, et al. Epithelial SOX9 drives progression and metastases of gastric adenocarcinoma by promoting immunosuppressive tumour microenvironment. *Gut.* 2023;72(4):624–37.
14. Jiang Y, Wang Y, Chen G, Sun F, Wu Q, Huang Q et al. Nicotinamide metabolism face-off between macrophages and fibroblasts manipulates the micro-environment in gastric cancer. *Cell Metab.* 2024;36(8):1806–1822.e11.
15. Shinya Umekita D, Kiyozawa K, Kohashi S, Kawatoko T, Sasaki E, Ihara, et al. Clinicopathological significance of microsatellite instability and immune escape mechanism in patients with gastric solid-type poorly differentiated adenocarcinoma. *Gastric Cancer.* 2024;27(3):484–94.
16. Tang Y, Cui G, Liu H, Han Y, Cai C, Feng Z, et al. Converting cold to hot: epigenetics strategies to improve immune therapy effect by regulating tumor-associated immune suppressive cells. *Cancer Commun (Lond).* 2024;44(6):601–36.
17. Shogo Kumagai S, Koyama K, Itahashi T, Tanegashima Y-T, Lin Y, Togashi, et al. Lactic acid promotes PD-1 expression in regulatory T cells in highly glycolytic tumor microenvironments. *Cancer Cell.* 2022;40(2):201–. – 18.e9.
18. Shogo Kumagai K, Itahashi H, Nishikawa. Regulatory T cell-mediated immunosuppression orchestrated by cancer: towards an immuno-genomic paradigm for precision medicine. *Nat Rev Clin Oncol.* 2024;21(5):337–53.
19. Kota Itahashi T, Irie H, Nishikawa. Regulatory T-cell development in the tumor microenvironment. *Eur J Immunol.* 2022;52(8):1216–27.
20. Tanaka A. Shimon Sakaguchi. Regulatory T cells in cancer immunotherapy. *Cell Res.* 2017;27(1):109–18.
21. Chen Q, Shen M, Han MYX, Mu S, Li Y, et al. Targeting tumor-infiltrating CCR8 + regulatory T cells induces antitumor immunity through functional restoration of CD4 + tconv and CD8 + T cells in colorectal cancer. *J Transl Med.* 2024;22(1):709.
22. Kamada T, Togashi Y, Tay C, Ha D, Sasaki A, Nakamura Y, et al. PD-1 + regulatory T cells amplified by PD-1 blockade promote hyperprogression of cancer. *Proc Natl Acad Sci U S A.* 2019;116(20):9999–10008.

23. Kumagai S, Togashi Y, Kamada T, Sugiyama E, Nishinakamura H, Takeuchi Y, et al. The PD-1 expression balance between effector and regulatory T cells predicts the clinical efficacy of PD-1 blockade therapies. *Nat Immunol*. 2020;21(11):1346–58.
24. Kenro Tanoue H, Ohmura K, Uehara M, Ito K, Yamaguchi K, Tsuchihashi, et al. Spatial dynamics of CD39 + CD8 + exhausted T cell reveal tertiary lymphoid structures-mediated response to PD-1 blockade in esophageal cancer. *Nat Commun*. 2024;15(1):9033.
25. Xu Liu D, Xu C, Huang Y, Guo S, Wang C, Zhu, et al. Regulatory T cells and M2 macrophages present diverse prognostic value in gastric cancer patients with different clinicopathologic characteristics and chemotherapy strategies. *J Transl Med*. 2019;17(1):192.
26. Xu Liu Z, Zhang G, Zhao. Recent advances in the study of regulatory T cells in gastric cancer. *Int Immunopharmacol*. 2019;73:560–67.
27. Ion, Negura. Mariana Pavel-Tanasa, Mihai Danciu. Regulatory T cells in gastric cancer: key controllers from pathogenesis to therapy. *Cancer Treat Rev*. 2023;120:102629.
28. Shannon N, Geels A, Moshensky RS, Sousa C, Murat MA, Bustos BL, Walker, et al. Interruption of the intratumor CD8 + T cell:Treg crosstalk improves the efficacy of PD-1 immunotherapy. *Cancer Cell*. 2024;42(6):1051–e667.
29. Thomas Denize OA, Jegede S, Matar NE, Ahmar, Destiny J, West E, Walton, et al. PD-1 expression on Intratumoral Regulatory T Cells Is Associated with Lack of Benefit from Anti-PD-1 Therapy in Metastatic Clear-Cell Renal Cell Carcinoma patients. *Clin Cancer Res*. 2024;30(4):803–13.
30. Ton N, Schumacher, Daniela S, Thommen. Tertiary lymphoid structures in cancer. *Science*. 2022;375(6576):eabf9419.
31. Teillaud J-L, Houel A, Panouillot M, et al. Tertiary lymphoid structures in anticancer immunity. *Nat Rev Cancer*. 2024;24(9):629–46.
32. Catherine Sautès-Fridman F, Petitprez J, Calderaro. Wolf Herman Fridman. Tertiary lymphoid structures in the era of cancer immunotherapy. *Nat Rev Cancer*. 2019;19(6):307–25.
33. Chupeng H, You W, Kong D, Huang Y, Lu JY, Zhao M, et al. Tertiary lymphoid structure-Associated B cells enhance CXCL13 + CD103 + CD8 + tissue-Resident memory T-Cell response to programmed cell death protein 1 blockade in Cancer Immunotherapy. *Gastroenterology*. 2024;166(6):1069–84.
34. Chen Y, Jia K, Sun Y, Zhang C, Li Y, Zhang L, et al. Predicting response to immunotherapy in gastric cancer via multi-dimensional analyses of the tumour immune microenvironment. *Nat Commun*. 2022;13(1):4851.
35. Yingying Wu J, Zhao Z, Wang D, Liu C, Tian B, Ye, et al. Association of systemic inflammatory markers and tertiary lymphoid structure with pathological complete response in gastric cancer patients receiving preoperative treatment: a retrospective cohort study. *Int J Surg*. 2023;109(12):4151–61.
36. Shu Yazaki T, Shimoi M, Yoshida H, Sumiyoshi-Okuma M, Arakaki A, Saito, et al. Integrative prognostic analysis of tumor-infiltrating lymphocytes, CD8, CD20, programmed cell death-ligand 1, and tertiary lymphoid structures in patients with early-stage triple-negative breast cancer who did not receive adjuvant chemotherapy. *Breast Cancer Res Treat*. 2023;197(2):287–97.
37. Quan Jiang C, Tian H, Wu L, Min H, Chen L, Chen, et al. Tertiary lymphoid structure patterns predicted anti-PD1 therapeutic responses in gastric cancer. *Chin J Cancer Res*. 2022;34(4):365–82.
38. Lenka Kasikova J, Rakova M, Hensler T, Lanickova J, Tomankova J, Pasulka, et al. Tertiary lymphoid structures and B cells determine clinically relevant T cell phenotypes in ovarian cancer. *Nat Commun*. 2024;15(1):2528.
39. Hui Z, Zhang J, Ren Y, Li X, Yu CYW, et al. Single-cell profiling of immune cells after neoadjuvant pembrolizumab and chemotherapy in IIIA non-small cell lung cancer (NSCLC). *Cell Death Dis*. 2022;13(7):607.
40. Sadeghirad H, Monkman J, Tan CW, Liu N, Yunis J, Meg L, Donovan, et al. Spatial dynamics of tertiary lymphoid aggregates in head and neck cancer: insights into immunotherapy response. *J Transl Med*. 2024;22(1):677.
41. Danaher P, Warren S, Dennis L, White LDAA, Disis ML, et al. Gene expression markers of Tumor infiltrating leukocytes. *J Immunother Cancer*. 2017;5:18.
42. Michael S, Rooney SA, Shukla CJ, Wu G, Getz, Nir Hacohen. Molecular and genetic properties of tumors associated with local immune cytolytic activity. *Cell*. 2015;160(1–2):48–61.
43. Dvir A, Atul ZH, Butte J. xCell: digitally portraying the tissue cellular heterogeneity landscape. *Genome Biol*. 2017;18(1):220.
44. Ayers M, Lunceford J, Nebozhyn M, Murphy E, Loboda A, Kaufman DR, et al. IFN- $\gamma$ -related mRNA profile predicts clinical response to PD-1 blockade. *J Clin Invest*. 2017;127(8):2930–40.
45. Lauss RCM, Sanna A, Donia M, Larsen MS, Mitra S, Johansson I, et al. Tertiary lymphoid structures improve immunotherapy and survival in melanoma. *Nature*. 2020;577(7791):561–65.
46. Tongbo Wang N, Wang H, Zhou A, Zhou J, Jin Y, Chen, et al. Long-term survival results of patients with locally advanced gastric cancer and pathological complete response after neoadjuvant chemotherapy and resection. *Transl Cancer Res*. 2020;9(2):529–35.
47. Xu S, Zhu Q, Wu L, Wang Y, Wang J, Zhu L et al. Association of the CD4+/CD8+ ratio with response to PD-1 inhibitor-based combination therapy and dermatological toxicities in patients with advanced gastric and esophageal cancer. *Int Immunopharmacol*. 2023;123:110642.
48. Wang HQ, Mulford LJ, Sharp F, Liang J, Kurtulus S, Trabucco G, et al. Inhibition of MDM2 promotes antitumor responses in p53 wild-type Cancer cells through their Interaction with the Immune and Stromal Microenvironment. *Cancer Res*. 2021;81(11):3079–91.
49. Jiang Liu D, Liu G, Wang HJ, Chen D, Song C, et al. Circulating memory PD-1 + CD8 + T cells and PD-1 + CD8 + T/PD-1 + CD4 + T cell ratio predict response and outcome to immunotherapy in advanced gastric cancer patients. *Cancer Cell Int*. 2023;23(1):274.
50. Daniel H, Shu WJ, Ho, Luciane T, Kagohara A, Gargis SM, Shin L, Danilova, et al. Immunotherapy response induces divergent tertiary lymphoid structure morphologies in hepatocellular carcinoma. *Nat Immunol*. 2024;25(11):2110–23.
51. Chen C, Han J, He Q, Yao Q, Wang X, Peng Z, et al. Tumor-infiltrating immune cell profiles and changes associate with additional trastuzumab in preoperative chemotherapy for patients with HER2-positive gastric cancer. *Br J Cancer*. 2024;131(9):1463–72.
52. Luise Rupp I, Dietsche M, Kiebler U, Sommer A, Muckenhuber K, Steiger, et al. Neoadjuvant chemotherapy is associated with suppression of the B cell-centered immune landscape in pancreatic ductal adenocarcinoma. *Front Immunol*. 2024;15:1378190.
53. Xiaoyan S, Liu W, Sun L, Mo H, Feng Y, Wu X, et al. Maturation and abundance of tertiary lymphoid structures are associated with the efficacy of neoadjuvant chemoimmunotherapy in resectable non-small cell lung cancer. *J Immunother Cancer*. 2022;10(11):e005531.
54. Siwei Zheng W, Wang L, Shen Y, Yao W, Xia, Chao Ni. Tumor battlefield within inflamed, excluded or desert immune phenotypes: the mechanisms and strategies. *Exp Hematol Oncol*. 2024;13(1):80.
55. Xiang X, Guo F, Li G, Ma L, Zhu X, Abdulla Z, et al. Efficacy of intra-arterial chemotherapy with sequential anti-PD-1 antibody in unresectable gastric cancer: a retrospective real-world study. *Front Oncol*. 2023;12:1015962.
56. Tessa S, Groen-van Schooten RF, Fernandez, Nicole CT, van Grieken EN, Bos J, Seidel J, Saris, et al. Mapping the complexity and diversity of tertiary lymphoid structures in primary and peritoneal metastatic gastric cancer. *J Immunother Cancer*. 2024;12(7):e009243.
57. Huang KC-Y, Chiang S-F, Lin P-C, Hong W-Z, Yang P-C. TNF $\alpha$  modulates PAX1 activation to promote ATP release and enhance P2RX7-mediated antitumor immune responses after chemotherapy in colorectal cancer. *Cell Death Dis*. 2024;15(1):24.
58. Yu Y-P, Cai L-C, Wang X-Y, Cheng S-Y, Zhang D-M, Jian W-G, et al. BMP8A promotes survival and drug resistance via Nrf2/TRIM24 signaling pathway in clear cell renal cell carcinoma. *Cancer Sci*. 2020;111(5):1555–66.
59. Jinfen Wei M, Huang HK, Lin S, Hongli Du. Roles of proteoglycans and glycosaminoglycans in Cancer Development and Progression. *Int J Mol Sci*. 2020;21(17):5983.
60. Simone Allegrini M, Camici M, Garcia-Gil R, Pesì. Maria Grazia Tozzi. Interplay between mTOR and Purine Metabolism Enzymes and its relevant Role in Cancer. *Int J Mol Sci*. 2024;25(12):6735.
61. Carter William C, Wangmo A, Ranjan. Unravelling the application of machine learning in cancer biomarker discovery. *Cancer Insight*. 2023; 2(1).
62. Fatemeh Movahedi L, Li ZP. Xu. Repurposing anti-parasite benzimidazole drugs as selective anti-cancer chemotherapeutics. *Cancer Insight*. 2023; 2(1).
63. Nurumal SR, Ramli NS, Zulkefley Mohammad, Shamsul Azhar Shah. Traditional herbal medicine as adjunctive therapy for colorectal cancer: a scoping review. *Traditional Med Res*. 2022;7(2):15.
64. Ji X, Tian X, Feng S, Zhang L, Wang J, Guo R et al. Intermittent F-actin perturbations by magnetic fields inhibit breast Cancer metastasis. *Research (Wash D C)*. 2023;6:0080.
65. Liang H, Lu Q, Yang J. Guocan Yu. Supramolecular Biomaterials for Cancer Immunotherapy. *Research (Wash D C)*. 2023;6:0211.

## Publisher's note

Springer Nature remains neutral with regard to jurisdictional claims in published maps and institutional affiliations.